Non-Markovian effects on quantum beats

J. P. Lavoine, A. J. Boeglin, P. Martin, and A. A. Villaeys
Institut de Physique et Chimie des Matériaux de Strasbourg Groupe d'Optique Nonlinéaire et d'Optoélectronique, 23, rue du Loess, 67037 Strasbourg Cedex, France
(Received 22 November 1995)

The transient four-wave mixing signal from a three-level system coupled to a bath of harmonic oscillators is calculated in the short-pulse limit. This allows an examination of the non-Markovian effects on the relaxation processes in the excited levels between which beating occurs. In particular, it is possible to distinguish between oscillations which are due to oscillatory dephasing, a consequence of the memory effects, and oscillations due to the quantum beats. This also allows one to analyze how these two kinds of oscillations are mixed together. We show that we not only have an amplitude modulation of the beats as in the Markovian case but also deformations of the beats for short delays between the exciting light pulses. These deformations are a consequence of the nonequilibrium motion of the surroundings of the system under optical excitation.

I. INTRODUCTION

These last years have seen an important development in the use of femtosecond light pulses to study induced nuclear vibrational motion in molecules.[1–3] The motion induced by an ultrashort light pulse gives rise to an oscillatory modulation in the transient absorption of the molecule, which can be measured by pump-probe techniques.[4,5] These oscillations or quantum beats have also been observed in transient four-wave mixing (TFWM) experiments such as photon-echo experiments.[3,6,7] They result from a quantum-mechanical coherent superposition of several discrete but close-lying states. It has been shown that it is possible to determine homogeneous linewidths of vibrational transitions in either the ground or the excited electronic state from such data.[4,5] From the theoretical standpoint, it is generally assumed that the relaxation processes of the media under investigation can be described by time-independent constants which are then extracted from the oscillations in the detected signal by fitting them with the predictions from an appropriate level scheme. Even recently, it has been proposed to improve on this basic approach by considering the possibility of correlations in the inhomogeneous broadening of the close-lying transitions, while keeping the basic concept of relaxation constants.[8]

With the recent progress in ultrafast optical techniques, ever shorter light pulses are being used in these nonlinear experiments. On such ultrashort time scales, phase relaxation can no longer be properly descibed by a time-independant dephasing time T_2.[9–11] It is now well established that non-Markovian effects due to thermal reservoir memory have an important bearing on the analysis of TFWM experiments.[12–18] As shown in Aihara's work,[15] non-Markovian relaxation is not only characterized by a nonexponential decay of the signal intensity but also by an oscillatory dephasing. These oscillations are not quantum beats. They are due to the dynamics of the reservoir motion and this phenomena should be interpreted as a non-Markovian effect.[18] In this context one question becomes important: What happens if we consider a TFWM experiment in a short-time regime where non-Markovian effects play a role while the excited material should exhibit quantum beats in such experiments. This is the goal of this paper. This point seems crucial because, as already mentioned, quantum beats result from a quantum-mechanical coherent superposition of discrete states. But this coherent superposition depends on the dephasing processes of the involved states. If these dephasing processes present also an oscillatory behavior, it is important to know how quantum beats will be affected by these non-Markovian effects.

From a theoretical standpoint, non-Markovian effects have been the subject of a number of works.[19–23] The theoretical approaches can be divided into two groups. One is called the stochastic model[24,25] and the other the microscopic model.[26] The stochastic model has been widely used to describe TFWM experiments in molecules in solution. It considers that the surroundings of the studied material can be modeled by a frequency modulation of the material levels. This modulation is treated as a stationary random process. In this approach, the reservoir does not appear explicitly but the situation being described corresponds implicitly to that of a thermal bath remaining in the same state of dynamical equilibrium throughout the experiment. The nonequilibrium motion of the surroundings of the system under optical excitation cannot be describe by this approach, whereas for our purpose, it will be essential to find out whether non-Markovian effects will affect the beat frequency by, for example, making it change over time. This would correspond to an identifiable nonequilibrium situation and therefore the microscopic approach has been chosen to describe the surroundings.

II. THEORY

We consider the simplest system for which quantum beats appear, namely, a three-level system as shown schematically in Fig. 1. The excited state is assumed to consist of two sublevels 2 and 3. Optical transitions from the ground-state level 1 to both levels 2 and 3 are allowed. This system is in interaction with its surroundings (bath) which is described by a set of harmonic oscillators. This model is typically used in

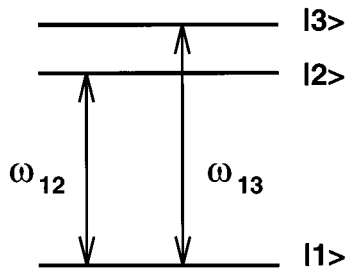

FIG. 1. Three-level system.

the description of a localized-electron–phonon system.[27–31] We shall use this terminology in the following but it must be kept in mind that this approach is quite general and can be applied to various kinds of systems. The full Hamiltonian can be written as

$$H_0 = H_{11}|1\rangle\langle 1| + H_{22}|2\rangle\langle 2| + H_{33}|3\rangle\langle 3|, \tag{2.1}$$

with

$$H_{11} = \sum_k \hbar\omega_k (b_k^\dagger b_k + \tfrac{1}{2}), \tag{2.2}$$

$$H_{22} = H_{11} + \hbar\omega_2 + V_2, \tag{2.3}$$

$$H_{33} = H_{11} + \hbar\omega_3 + V_3, \tag{2.4}$$

where b_k ($b_k^\dagger$) is the annihilation (creation) operator for the kth phonon mode with frequency ω_k, and where $\hbar\omega_2$ and $\hbar\omega_3$ are the electronic excitation energies. The electron-phonon interaction Hamiltonians V_i, for $i = 2,3$ are expressed as[15]

$$V_i = \sum_k h_k^{(i)} \omega_k (b_k + b_k^\dagger) + \frac{1}{2}\sum_k \sum_q h_{k,q}^{(i)} \sqrt{\omega_k \omega_q}\,(b_k + b_k^\dagger) \times (b_q + b_q^\dagger). \tag{2.5}$$

The first and second terms in Eq. (2.5) describe the linear and quadratic interactions, and $h_k^{(i)}$ and $h_{k,q}^{(i)}$ are their dimensionless interaction constants. We assume that they are independent of the modes. Therefore we write

$$\forall k, \quad h_k^{(i)} = h_L^{(i)}, \quad \text{and} \quad \forall k,q, \quad h_{k,q}^{(i)} = h_Q^{(i)}, \tag{2.6}$$

where the constant indices L and Q indicate the linear part or the quadratic part of the interaction. In this theoretical model, these interaction constants depend only on sublevel 2 or 3.

This system is in interaction with an electric field and the matter-radiation interaction Hamiltonian is given in the dipole approximation by

$$H_1(\boldsymbol{r},t) = -\boldsymbol{\mu}\cdot\boldsymbol{E}(\boldsymbol{r},t), \tag{2.7}$$

where $\boldsymbol{\mu}$ is the dipole-moment operator which can be written as

$$\boldsymbol{\mu} = \begin{pmatrix} 0 & \boldsymbol{\mu}_{12} & \boldsymbol{\mu}_{13} \\ \boldsymbol{\mu}_{21} & 0 & 0 \\ \boldsymbol{\mu}_{31} & 0 & 0 \end{pmatrix}. \tag{2.8}$$

We assume for simplicity that

$$\boldsymbol{\mu}_{12} = \boldsymbol{\mu}_{21} = \boldsymbol{\mu}_2 \quad \text{and} \quad \boldsymbol{\mu}_{13} = \boldsymbol{\mu}_{31} = \boldsymbol{\mu}_3, \tag{2.9}$$

and that $\boldsymbol{\mu}$ is independent of bath variables. Finally $\boldsymbol{E}(\boldsymbol{r},t)$ is the electric field in the material and takes the general form

$$\boldsymbol{E}(\boldsymbol{r},t) = \sum_\alpha \{\mathscr{E}_\alpha(t)\exp[i(\omega t - \boldsymbol{k}_\alpha\cdot\boldsymbol{r})] + \text{c.c.}\}. \tag{2.10}$$

Starting from the master equation for the density matrix ρ,

$$\frac{d\rho}{dt} = -\frac{i}{\hbar}[H_0 + H_1(\boldsymbol{r},t), \rho], \tag{2.11}$$

the equations of motion for the elements of the density matrix are obtained by using a perturbative approach up to the third order. We assume that the initial conditions correspond to

$$\rho(-\infty) = |1\rangle\langle 1|\rho_R, \tag{2.12}$$

where

$$\rho_R = \exp(-\beta H_{11})/\mathrm{Tr}[\exp(-\beta H_{11})]. \tag{2.13}$$

It is important to note that ρ in Eq. (2.11) represents the total density matrix of the material-bath system. The induced polarization $\boldsymbol{P}$ which is the source term in Maxwell's equations for the radiated field is

$$\boldsymbol{P} = \mathrm{Tr}_{\text{material}}[\mathrm{Tr}_{\text{bath}}[\boldsymbol{\mu}\rho]] \tag{2.14}$$

$$= \mathrm{Tr}_{\text{material}}[\boldsymbol{\mu}\sigma] \tag{2.15}$$

$$= \boldsymbol{\mu}_2\sigma_{21} + \boldsymbol{\mu}_3\sigma_{31} + \text{c.c.}, \tag{2.16}$$

where σ is the reduced density matrix obtained by

$$\sigma = \mathrm{Tr}_{\text{bath}}[\rho]. \tag{2.17}$$

Then the third-order perturbative solution of Eq. (2.11) combined with Eq. (2.17) leads to the following expressions for the nondiagonal elements σ_{12}:

$$\sigma_{12}^{(3)}(\boldsymbol{r},t)=\frac{i\mu_2^3}{\hbar^3}\int_{-\infty}^{t}dt_1\int_{-\infty}^{t_1}dt_2\int_{-\infty}^{t_2}dt_3E(\boldsymbol{r},t_1)E(\boldsymbol{r},t_2)E(\boldsymbol{r},t_3)\mathrm{Tr}_{\mathrm{bath}}\Bigg\{\Bigg[\exp\Big(-\frac{i}{\hbar}H_0^{11}(t-t_1)\Big)\exp\Big(-\frac{i}{\hbar}H_0^{22}(t_1-t_3)\Big)\rho_R$$
$$\times\exp\Big(\frac{i}{\hbar}H_0^{11}(t_2-t_3)\Big)\exp\Big(\frac{i}{\hbar}H_0^{22}(t-t_2)\Big)\Bigg]+\Bigg[\exp\Big(-\frac{i}{\hbar}H_0^{11}(t-t_1)\Big)\exp\Big(-\frac{i}{\hbar}H_0^{22}(t_1-t_2)\Big)$$
$$\times\exp\Big(-\frac{i}{\hbar}H_0^{11}(t_2-t_3)\Big)\rho_R\exp\Big(\frac{i}{\hbar}H_0^{22}(t-t_3)\Big)\Bigg]+\Bigg[\exp\Big(-\frac{i}{\hbar}H_0^{11}(t-t_2)\Big)\exp\Big(-\frac{i}{\hbar}H_0^{22}(t_2-t_3)\Big)\rho_R$$
$$\times\exp\Big(\frac{i}{\hbar}H_0^{11}(t_1-t_3)\Big)\exp\Big(\frac{i}{\hbar}H_0^{22}(t-t_1)\Big)\Bigg]+\Bigg[\exp\Big(-\frac{i}{\hbar}H_0^{11}(t-t_3)\Big)\rho_R\exp\Big(\frac{i}{\hbar}H_0^{22}(t_2-t_3)\Big)\exp\Big(\frac{i}{\hbar}H_0^{11}(t_1-t_2)\Big)$$
$$\times\exp\Big(\frac{i}{\hbar}H_0^{22}(t-t_1)\Big)\Bigg]\Bigg\}+\frac{i\mu_2\mu_3^2}{\hbar^3}\int_{-\infty}^{t}dt_1\int_{-\infty}^{t_1}dt_2\int_{-\infty}^{t_2}dt_3E(\boldsymbol{r},t_1)E(\boldsymbol{r},t_2)E(\boldsymbol{r},t_3)\mathrm{Tr}_{\mathrm{bath}}\Bigg\{\Bigg[\exp\Big(-\frac{i}{\hbar}H_0^{11}(t-t_2)\Big)$$
$$\times\exp\Big(-\frac{i}{\hbar}H_0^{33}(t_2-t_3)\Big)\rho_R\exp\Big(\frac{i}{\hbar}H_0^{11}(t_1-t_3)\Big)\exp\Big(\frac{i}{\hbar}H_0^{22}(t-t_1)\Big)\Bigg]+\Bigg[\exp\Big(-\frac{i}{\hbar}H_0^{11}(t-t_3)\Big)\rho_R$$
$$\times\exp\Big(\frac{i}{\hbar}H_0^{33}(t_2-t_3)\Big)\exp\Big(\frac{i}{\hbar}H_0^{11}(t_1-t_2)\Big)\exp\Big(\frac{i}{\hbar}H_0^{22}(t-t_1)\Big)\Bigg]+\Bigg[\exp\Big(-\frac{i}{\hbar}H_0^{11}(t-t_1)\Big)\exp\Big(-\frac{i}{\hbar}H_0^{33}(t_1-t_2)\Big)$$
$$\times\exp\Big(-\frac{i}{\hbar}H_0^{11}(t_2-t_3)\Big)\rho_R\exp\Big(\frac{i}{\hbar}H_0^{22}(t-t_3)\Big)\Bigg]+\Bigg[\exp\Big(-\frac{i}{\hbar}H_0^{11}(t-t_1)\Big)\exp\Big(-\frac{i}{\hbar}H_0^{33}(t_1-t_3)\Big)\rho_R$$
$$\times\exp\Big(\frac{i}{\hbar}H_0^{11}(t_2-t_3)\Big)\exp\Big(\frac{i}{\hbar}H_0^{22}(t-t_2)\Big)\Bigg]\Bigg\}. \tag{2.18}$$

Notice that $\sigma_{13}^{(3)}(\boldsymbol{r},t)$ is obtained by exchanging the indices 2 and 3 in the above expression. Here, $\boldsymbol{E}(\boldsymbol{r},t)$ appears as a scalar quantity because we have assumed that the exciting fields are all linearly polarized. Therefore, the vector nature of $\boldsymbol{E}(\boldsymbol{r},t)$, $\boldsymbol{\mu}_1$, and $\boldsymbol{\mu}_2$ can be omitted. In other respects, the terms H_0^{ii} represent the element $\langle i|H_0|i\rangle$ which is an operator in the bath space. At this step of the calculation it is necessary to evaluate the different trace operations which appear in the expressions. All the trace operations which appear in expression (2.18) can be performed provided that one can evaluate the general term

$$\mathrm{Tr}_{\mathrm{bath}}\Big[\exp\Big(\frac{i}{\hbar}H_0^{11}\tau_1\Big)\exp\Big(\frac{i}{\hbar}H_0^{mm}\tau_2\Big)\exp\Big(\frac{i}{\hbar}H_0^{11}\tau_3\Big)\exp\Big(-\frac{i}{\hbar}H_0^{nn}(\tau_1+\tau_2+\tau_3)\Big)\rho_R\Big], \tag{2.19}$$

for m and n varying between 2 and 3.

After some straightforward algebra, such an expression can be expressed as

$$\exp(i\omega_{mm}\tau_2)\exp\{-[i\omega_{nn}(\tau_1+\tau_2+\tau_3)]\}\exp[K_{mn}(\tau_1,\tau_2,\tau_3)], \tag{2.20}$$

where $K_{mn}(\tau_1,\tau_2,\tau_3)$ is simply evaluated by the cumulant expansion method up to the second order. We obtain

$$K_{mn}(\tau_1,\tau_2,\tau_3)=-\frac{i}{\hbar}\langle V_{nn}\rangle(\tau_1+\tau_2+\tau_3)+\frac{i}{\hbar}\langle V_{mm}\rangle\tau_2-\frac{1}{\hbar^2}\int_0^{\tau_1+\tau_2+\tau_3}ds_1\int_0^{s_1}ds_2\{\langle V_{nn}(s_1)V_{nn}(s_2)\rangle-\langle V_{nn}\rangle^2\}$$
$$+\frac{1}{\hbar^2}\int_0^{\tau_2}ds_1\int_0^{\tau_1+\tau_2+\tau_3}ds_2\{\langle V_{mm}(s_1+\tau_1)V_{nn}(s_2)\rangle-\langle V_{mm}V_{nn}\rangle\}-\frac{1}{\hbar^2}\int_0^{\tau_2}ds_1\int_0^{s_1}ds_2\{\langle V_{mm}(s_2)V_{mm}(s_1)\rangle$$
$$-\langle V_{mm}\rangle^2\} \tag{2.21}$$

$$=-\frac{i}{\hbar}\langle V_{nn}\rangle(\tau_1+\tau_2+\tau_3)+\frac{i}{\hbar}\langle V_{mm}\rangle\tau_2+Q_{mn}(\tau_1,\tau_2,\tau_3), \tag{2.22}$$

where $\langle\cdots\rangle$ denotes $\mathrm{Tr}_{\mathrm{bath}}[\cdots\rho_R]$. $V_{nn}(s)$ corresponds to V_{nn} in the interaction picture. Using Eq. (2.5), $Q_{mn}(\tau_1,\tau_2,\tau_3)$ can be written as

$$Q_{mn}(\tau_1,\tau_2,\tau_3)=R_{mn}(\tau_1,\tau_2,\tau_3)+iI_{mn}(\tau_1,\tau_2,\tau_3), \tag{2.23}$$

where

$$R_{mn}(\tau_1,\tau_2,\tau_3)=-[h_L^{(n)}]^2 g_L(\tau_1+\tau_2+\tau_3)-[h_L^{(m)}]^2 g_L(\tau_2)+h_L^{(m)}h_L^{(n)}[g_L(\tau_1+\tau_2)+g_L(\tau_2+\tau_3)-g_L(\tau_3)-g_L(\tau_1)]$$
$$-\frac{1}{2}[h_Q^{(n)}]^2 g_Q(\tau_1+\tau_2+\tau_3)-\frac{1}{2}[h_Q^{(m)}]^2 g_Q(\tau_2)+\frac{1}{2}h_Q^{(m)}h_Q^{(n)}[g_Q(\tau_1+\tau_2)+g_Q(\tau_2+\tau_3)-g_Q(\tau_3)-g_Q(\tau_1)] \tag{2.24}$$

and

$$I_{mn}(\tau_1,\tau_2,\tau_3)=[h_L^{(n)}]^2 g_L'(\tau_1+\tau_2+\tau_3)-[h_L^{(m)}]^2 g_L'(\tau_2)+h_L^{(m)}h_L^{(n)}[g_L'(\tau_2+\tau_3)+g_L'(\tau_1)-g_L'(\tau_3)-g_L'(\tau_1+\tau_2)]$$
$$+\frac{1}{2}[h_Q^{(n)}]^2 g_Q'(\tau_1+\tau_2+\tau_3)-\frac{1}{2}[h_Q^{(m)}]^2 g_Q'(\tau_2)+\frac{1}{2}h_Q^{(m)}h_Q^{(n)}[g_Q'(\tau_2+\tau_3)+g_Q'(\tau_1)-g_Q'(\tau_3)-g_Q'(\tau_1+\tau_2)]. \tag{2.25}$$

The functions $g_L(\tau)$, $g_Q(\tau)$, $g_L'(\tau)$, and $g_Q'(\tau)$ verify the relations

$$g_L(\tau)=\sum_k\,[1+2n(\omega_k)][1-\cos\omega_k\tau], \tag{2.26}$$

$$g_Q(\tau)=\sum_k\sum_q\left\{\{[1+n(\omega_k)][1+n(\omega_q)]+n(\omega_k)n(\omega_q)\}\frac{\omega_k\omega_q}{(\omega_k+\omega_q)^2}\{1-\cos[(\omega_k+\omega_q)\tau]\}\right.$$
$$\left.+2n(\omega_k)[1+n(\omega_q)]\frac{\omega_k\omega_q}{(\omega_k-\omega_q)^2}\{1-\cos[(\omega_k-\omega_q)\tau]\}\right\}, \tag{2.27}$$

$$g_L'(\tau)=\sum_k\,[\omega_k\tau-\sin\omega_k\tau], \tag{2.28}$$

$$g_Q'(\tau)=\sum_k\sum_q\left\{[1+n(\omega_k)+n(\omega_q)]\frac{\omega_k\omega_q}{(\omega_k+\omega_q)^2}\{(\omega_k+\omega_q)\tau-\sin[(\omega_k+\omega_q)\tau]\}\right.$$
$$\left.-2n(\omega_k)[1+n(\omega_q)]\frac{\omega_k\omega_q}{(\omega_k-\omega_q)^2}\{(\omega_k-\omega_q)\tau-\sin[(\omega_k-\omega_q)\tau]\}\right\}, \tag{2.29}$$

where $n(\omega)$ is the Bose-Einstein distribution function. An examination of relation (2.23) shows that the coupling between the bath and the three-level sytem introduces not only a time-dependent dephasing but also a time-dependent frequency shift of sublevels 2 and 3. At this point of the calculation, we have not made any assumptions about the exciting fields and our theory can be applied to various experimental situations. In this paper, our purpose is to describe a TFWM experiment as represented in Fig. 2. Then, instead of the general electric field given by relation (2.10), we may use

$$E(\mathbf{r},t)=\mathscr{E}_1(t-\tau)\exp[i(\omega t-\mathbf{k}_1\cdot\mathbf{r})]$$
$$+\mathscr{E}_2(t)\exp[i(\omega t-\mathbf{k}_2\cdot\mathbf{r})]+\text{c.c.}, \tag{2.30}$$

where τ is the delay between the pump pulse $\mathscr{E}_1(t)$ and the proble pulse $\mathscr{E}_2(t)$. In the following, we shall only consider the case where $\tau\geqslant 0$. We shall also assume that these non-Markovian frequency drifts are small with respect to the transition frequencies ω_2 and ω_3 so that we can apply the rotating wave approximation. On the other hand, we shall also assume that the time variations of the field envelopes $\mathscr{E}_1(t)$ and $\mathscr{E}_2(t)$ are fast compared to the dynamics of the system. Then we can apply the approximation of δ pulses and perform all the integrations in relation (2.18) to calculate the macroscopic polarization by using relation (2.16). In the total expression of the polarization, only the terms with the wave vector $2\mathbf{k}_1-\mathbf{k}_2$ need to be considered. This particular contribution can be written as

$$P^{(3)}(t)=\mathscr{P}^{(3)}(t)\exp\{i[\omega t-(2\mathbf{k}_1-\mathbf{k}_2)\cdot\mathbf{r}]\}+\text{c.c.}, \tag{2.31}$$

where $\mathscr{P}^{(3)}(t)$, aside from unimportant multiplicative factors, takes the form

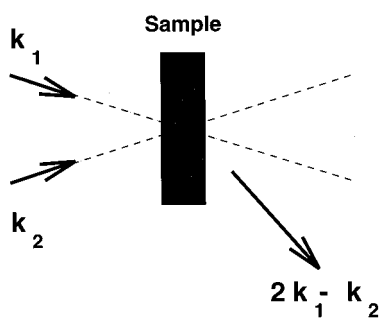

FIG. 2. Experimental configuration of a TFWM experiment.

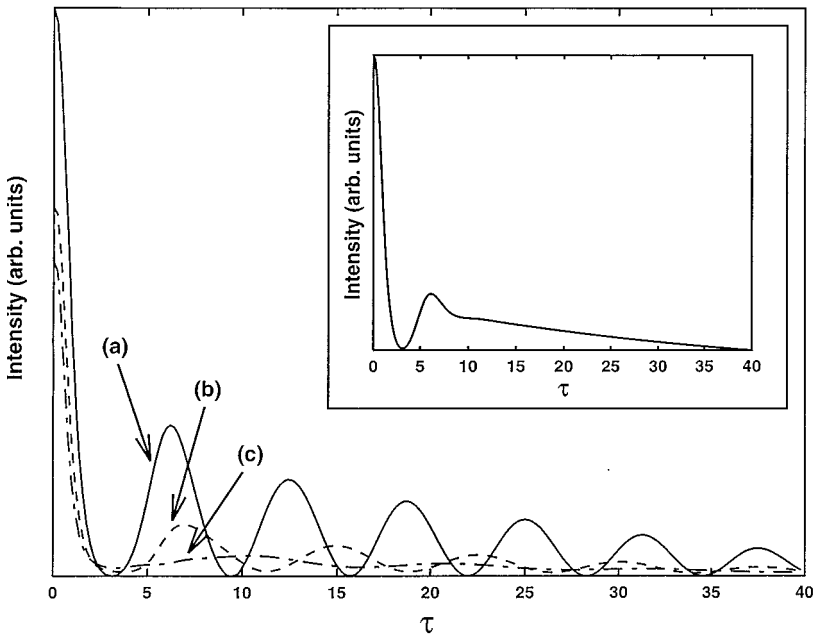

FIG. 3. Time-integrated intensity as a function of the pulse delay τ. The time axis is normalized by the phonon oscillation ω_p. For the three curves, $\beta=1$, $\gamma_p=0.4$, $\mu_2=\mu_3=1$, $h_L^{(2)}=0.4$, $h_Q^{(2)}=0.066$, $\Delta_2=0.5$, and $\Delta_3=-0.5$. Curve (a) is given for $h_L^{(2)}=h_L^{(3)}$ and $h_Q^{(2)}=h_Q^{(3)}$, (b) for $h_L^{(3)}=0.6$ and $h_Q^{(3)}=0.1$, and finally (c) corresponds to $h_L^{(3)}=0.8$, $h_Q^{(3)}=0.133$.

$$\mathscr{P}^{(3)}(t)=\mu_2^4\exp[i\Delta_2(t-2\tau)]\exp[Q_{22}(-\tau,\tau,t-\tau)/\hbar^2]+\mu_3^4\exp[i\Delta_3(t-2\tau)]\exp[Q_{33}(-\tau,\tau,t-\tau)/\hbar^2]$$
$$+\mu_3^2\mu_2^2\exp[i\Delta_3(t-\tau)]\exp[-i\Delta_2\tau]\exp[Q_{23}(-\tau,\tau,t-\tau)/\hbar^2]+\mu_3^2\mu_2^2\exp[i\Delta_2(t-\tau)]\exp[-i\Delta_3\tau]$$
$$\times\exp[Q_{32}(-\tau,\tau,t-\tau)/\hbar^2]. \tag{2.32}$$

Here, the quantities Δ_i, $i=2,3$, are equal to $\omega-\omega_i-\langle V_{ii}\rangle/\hbar$. Finally the intensity of radiation emitted in the direction $2\boldsymbol{k}_1-\boldsymbol{k}_2$ is given by

$$I(\tau)=\int_{-\infty}^{\infty}|\mathscr{P}^{(3)}(t)|^2dt. \tag{2.33}$$

III. SIMULATION

Before proceeding to simulations with our theoretical model, it is important to note that in the particular case where the sublevels have the same interaction constants,

$$h_L^{(2)}=h_L^{(3)},\quad h_Q^{(2)}=h_Q^{(3)}, \tag{3.1}$$

all the quantities $Q_{ij}(-\tau,\tau,t-\tau)$ are equal and can be factored out from expression (2.32). In this case, only the real part of Q contributes to the signal and we are left with an amplitude modulation of the beats. In the case where the interaction constants are different, the imaginary part of Q play also a role and the variation of the detected signal with respect to τ will be different. To study these effects, the integration which appears in relation (2.33) has been performed numerically and we have assumed that the phonon density of states has a Gaussian profile with maximum at ω_p and with width γ_p.[15] Then all the summations in the expressions (2.26) to (2.29) become standard integrations which are also evaluated numerically.

All the curves which will be presented represent the integrated intensity detected in the TFWM experiment for various parameters. The insets appearing on each plot display the amplitude modulation envelope; i.e., the amplitude of the quantum beats of the three-level system is modulated by the function sketched in the inset. Notice that the curves of the main graphs as well as of the insets have all arbitrarily been normalized to 1. The first simulation corresponds to Fig. 3 and Fig. 4. The difference between these curves lies in the energy gap between the two sublevels 2 and 3. Otherwise all the parameters are identical and correspond to the numerical simulation in Aihara's work.[15] As can be seen in the corresponding insets, the oscillations of the dephasing are not too important for this set of parameters. We have only one non-Markovian oscillation but it is useful, for now, to distinguish clearly the non-Markovian and Markovian parts of the integrated signal. Curves (a) correspond to same interaction constants (i.e., $h_L^{(2)}=h_L^{(3)}$ and $h_Q^{(2)}=h_Q^{(3)}$). In curves (b) and (c), we increase $h_L^{(3)}$ and $h_Q^{(3)}$ with respect to $h_L^{(2)}$ and $h_Q^{(2)}$ while the ratio h_L/h_Q is being held fixed.

An amplitude modulation is observed both in Fig. 3(a) and Fig. 4(a), but this appears more clearly in Fig. 4(a) where the quantum beat frequency is smaller than the one of the non-Markovian oscillation. In Fig. 3(a), they have been chosen so as to be of the same order.

The situation is different when the interaction constants are not equal as shown in curves (b) and (c) Fig. 3 or Fig. 4. We observe two phenomena. We notice first a difference in beat frequency which persists even in the Markovian part of the curves. This point is not surprising since it is due to the fact that we increase the interaction constants of level 3 and consequently the energy difference is also modified. The second phenomena is the appearance of deformations of the

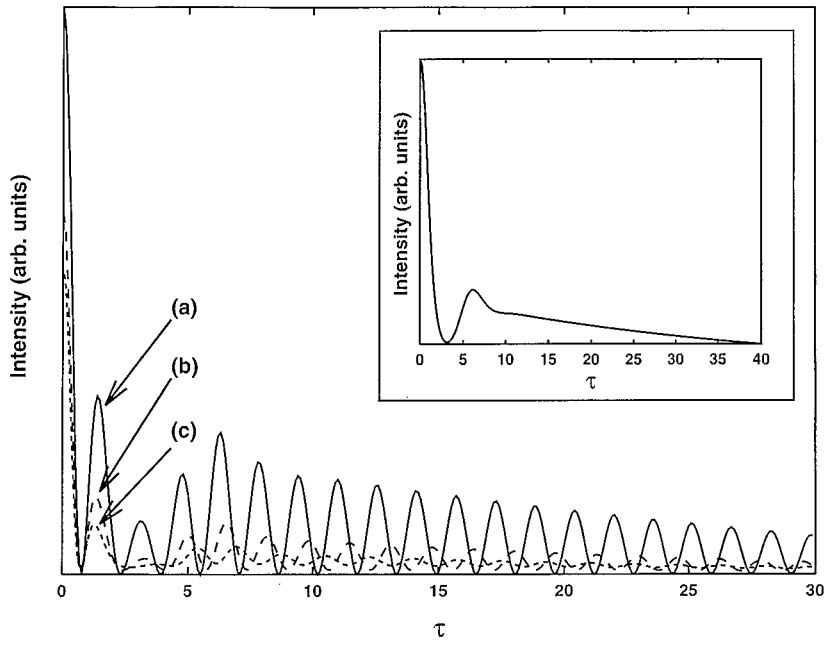

FIG. 4. Time-integrated intensity as a function of the pulse delay τ. The constants are identical to the ones taken in Fig. 3 except that here $\Delta_2=2$ and $\Delta_3=-2$.

beats but only for short delays which correspond to the non-Markovian part of the curves. The behavior is no longer sinusoidal as in the Markovian part and this is a consequence of the nonequilibrium motion of the bath. On a short-time scale we have a time dependence, and also a delay dependence, of the energy difference of the levels between which beating occurs. For short delays, we observe a non-Markovian behavior in the amplitude modulation of the beats but also in the delay dependence of the oscillation. Of course, for longer delays we find again a Markovian behavior as shown in Fig. 3 and Fig. 4. If we continue to increase the difference between the interaction constants, beating finally disappears.

The motivation behind the choice of the preceding set of parameters was to obtain curves sufficiently clear to distinguish the main physical phenomena but it is obvious that the oscillatory dephasing obtained in these simulated situations is not to be confused with quantum beats. Figures 5 and 6 illustrate a situation where the non-Markovian behavior leads to strong oscillations. Figure 5 corresponds to the same set of parameters as Fig. 4(a) except that we have taken a sharper phonon density to increase the oscillatory dephasing. We have only considered in this curve the case where the interactions constants are equal. Other simulations with increasing $h_L^{(3)}$ and $h_Q^{(3)}$ as in Figs. 4(b) and 4(c) do not show new phenomena and lead to very unreadable curves. Figure 5 shows clearly the modulation amplitude but, here the dephasing is highly oscillatory. Figure 6 corresponds to the same set of parameters as Fig. 3 but the phonon density is taken as in Fig. 5. Curves (a), (b), and (c) correspond to the same choice of interaction constants as that in Figs. 3(a), 3(b), and 3(c). Here, the beating period is of the same order than the non-Markovian oscillations. All the observed variations can be

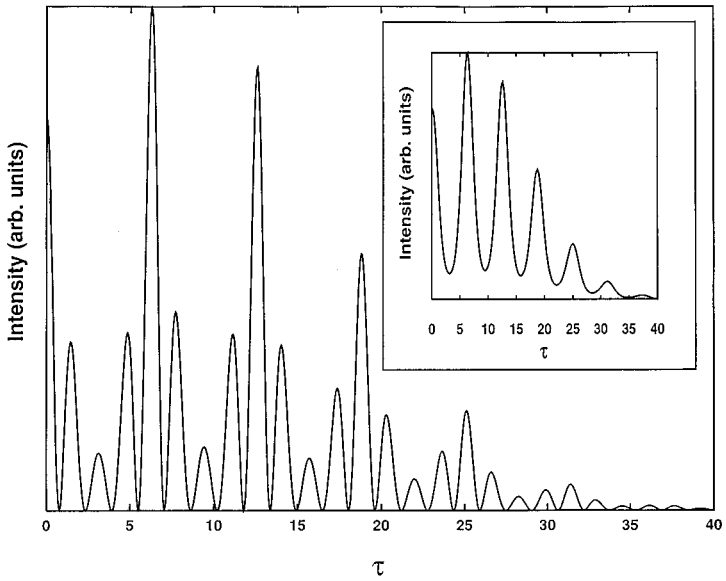

FIG. 5. Time-integrated intensity as a function of the pulse delay τ. The constants are identical to the ones taken in Fig. 4(a) except that here $\gamma_p=0.05$.

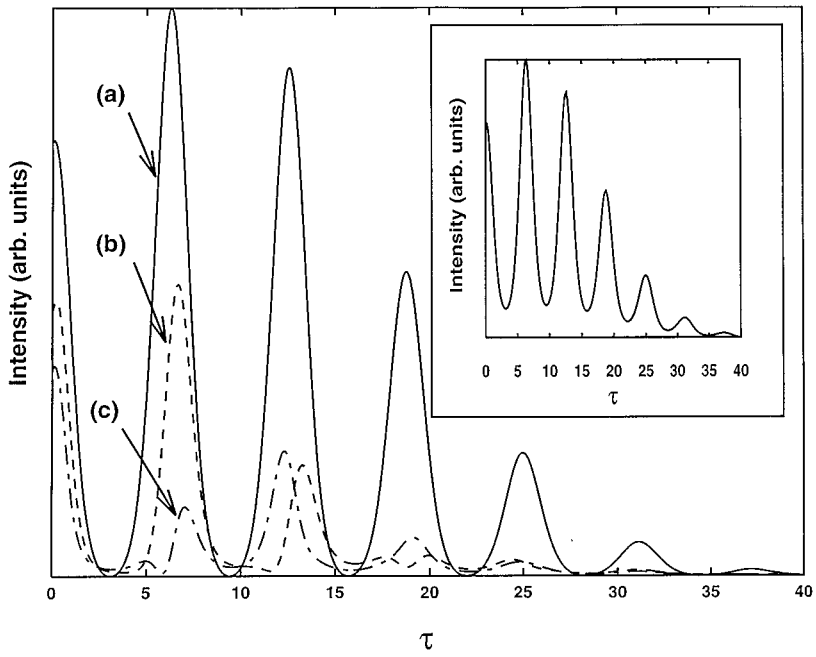

FIG. 6. Time-integrated intensity as a function of the pulse delay τ. The constants are identical to the ones taken in Fig. 3 except that here $\gamma_p = 0.05$.

explained with the same argument used for the situations illustrated in Fig. 3 or Fig. 4. Nevertheless, we see here that the surrounding nonequilibrium motion affects highly the beating when the interaction constants are different.

IV. CONCLUSION

To summarize, we have describe a TFWM experiment in a three-level system when quantum beats and non-Markovian effects occur simultaneously. Our theoretical approach is based on a microscopical description of the surroundings of the system under optical excitation by a set of harmonic oscillators. This model is not restricted to the description of localized-electron–phonon system but can be applied to various kind of materials. We have considered the case where memory effects induce an oscillatory dephasing. These non-Markovian oscillations must not be confused with quantum beats and we have analyzed how they affect the oscillations due to quantum beats. We have shown that a difference in the interaction constants between the levels and the bath leads to a deformation of the beats which are no longer harmonic for short delays between the light pulses. This anharmonicity is a consequence of the nonequilibrium motion of the surroundings. For equal interaction constants we have again found an amplitude modulation of the beats as in the Markovian case but the decay is not exponential for short delays. The deformations of the beats should be observable experimentally and are significant of the coupling difference between the bath and the levels between which beating occurs, making it possible to study the nonequilibrium motion of the surroundings of the system.

[1] J. Chesnoy and A. Mokhtari, Phys. Rev. A **38**, 3566 (1988).
[2] I.A. Walmsey, F.W. Wise, and C.L. Tang, Chem. Phys. Lett. **154**, 315 (1989).
[3] A. Tokmakoff, A.S. Kwok, R.S. Urdahl, R.S. Francis, and M.D. Fayer, Chem. Phys. Lett. **234**, 289 (1995).
[4] M. Mitsunaga and C.L. Tang, Phys. Rev. A **35**, 1720 (1987).
[5] I.A. Walmsey, M. Mitsunaga, and C.L. Tang, Phys. Rev. A **38**, 4681 (1988).
[6] L.Q. Lambert, Phys. Rev. B **7**, 1834 (1973).
[7] R.L. Schoemaker and F.A. Hopf, Phys. Rev. Lett. **33**, 1527 (1974).
[8] S.T. Cundiff, Phys. Rev. B **49**, 3114 (1994) and references therein.
[9] J.-Y. Bigot, M.T. Portella, R.W. Scoenlein, C.J. Bardeen, A. Migus, and C.V. Shank, Phys. Rev. Lett. **66**, 1138 (1991).
[10] Erik T.J. Nibbering, Douwe A. Wiersma, and Koos Duppen, Phys. Rev. Lett. **66**, 2464 (1991).
[11] P. Cong, Y.J. Yan, H.P. Deuel, and J.D. Simon, J. Chem. Phys. **100**, 7855 (1994).
[12] Eiichi Hanamura, J. Phys. Soc. Jpn. **52**, 2258 (1983).
[13] B.D. Fainberg, Opt. Spectrosc. (USSR) **55**, 669 (1983).
[14] M. Aihara, Phys. Rev. B **21**, 2051 (1980).
[15] M. Aihara, Phys. Rev. B **25**, 53 (1982).
[16] Shaul Mukamel, Phys. Rep. **93**, 1 (1982).
[17] Yosuke Kayanuma, Phys. Rev. B **41**, 3360 (1990).
[18] M. Aihara and M. Hama, Phys. Rev. B **52**, 3366 (1995).
[19] Shaul Mukamel, Chem. Phys. **37**, 33 (1979).
[20] P. Gligolini, Nuovo Cimento B **63**, 174 (1981).
[21] Y. Fujimura, T. Akiyama, T. Nakajima, H. Kono, and S.H. Lin, J. Chem. Phys. **84**, 2112 (1986).
[22] W. Vogel, D.-G. Welsch, and B. Wilhelmi, Phys. Rev. A **37**, 3825 (1988).
[23] A.A. Villaeys, J.C. Vallet, and S.H. Lin, Phys. Rev. A **43**, 5030 (1991).

[24] R. Kubo, J. Phys. Soc. Jpn. **17**, 1100 (1962).
[25] R. Kubo, J. Math. Phys. **4**, 174 (1963).
[26] J.L. Skinner and D. Hsu, J. Phys. Chem. **90**, 4931 (1986).
[27] V. Hizhnyakov and I. Tehver, Phys. Status Solidi **21**, 755 (1967).
[28] Y. Toyozawa, A. Kotani, and A. Sumi, J. Phys. Soc. Jpn. **42**, 1495 (1977).
[29] T. Takagahara, E. Hanamura, and R. Kubo, J. Phys. Soc. Jpn. **44**, 728 (1978).
[30] S. Mukamel, J. Chem. Phys. **73**, 5322 (1980).
[31] Y. Kayanuma, J. Phys. Soc. Jpn. **57**, 292 (1987).